The 2009 Horizontal Velocity Field for South America and the Caribbean

81

H. Drewes and O. Heidbach

Abstract

Station velocities derived from space geodetic measurements in Central and South America were processed by the finite element method using a geophysical model and by a least squares collocation approach with empirical correlation functions for computing a continuous velocity field of the South American and the Caribbean crust. Velocities of the reference frame for the Americas (SIRGAS), and of various geodynamic networks (CASA, SNAPP, CAP, SAGA, and seismic gap projects) are used as input data. In general, the results present good agreement with previous models. Moreover, there are significant improvements, particularly in areas with new data (northern and central Andes, southern Tierra del Fuego).

81.1 Introduction

A main objective of geodesy is the determination and representation of the geometry of the Earth surface and its variation with time, e.g. for the realization of reference frames, and the study of geodynamics and global change effects. The geophysical background model widely used for this purpose is the plate kinematic model NUVEL-1A (DeMets et al. 1990, 1994). However, this model represents only rigid plates and does not include deformation zones (such as the Andes). The geologic-geophysical model PB2002 (Bird 2003) includes deformation zones and a large number of (micro-) plates, but not all of these are confirmed by present-day geodetic measurements. In order to model the motions of the Earth crust for geodetic purposes we therefore need a realistic present-day crust deformation model.

The deformation of the South American crust is mainly due to the subduction of the Nazca Plate under the South America Plate (e.g. Espurt et al. 2008). This convergence of plates develops a broad deformation belt, as expressed by the growth of the Andes in the past 10 Ma (Heidbach et al. 2008). For geodetic purposes, e.g. for the transformation of station coordinates of observation sites without known velocities from one epoch to another, a continuous contemporary velocity field is essential. Such a field was first computed for the South American crust in 2003 (Drewes and Heidbach 2005). Since then, additional data sets from various geodetic and geodynamics projects have become available. They are used in the new computation presented here.

H. Drewes (✉)
Deutsches Geodätisches Forschungsinstitut, Alfons-Goppel-Str. 11, 80539 München, Germany
e-mail: drewes@dgfi.badw.de

O. Heidbach
GFZ German Research Centre for Geosciences, Telegrafenberg, 14473 Potsdam, Germany

S. Kenyon et al. (eds.), *Geodesy for Planet Earth*, International Association of Geodesy Symposia 136,
DOI 10.1007/978-3-642-20338-1_81,

81.2 Input Data

The input data for the present computation of the velocity field are taken from the following projects:

- One twenty eight station velocities (Fig. 81.1) of the multi-year GPS solution SIR09P01 of the International GNSS Service's (IGS) Regional Network Associate Analysis Center (RNAAC) for the Geocentric Reference System for the Americas (SIRGAS) at DGFI (Seemüller et al. 2009) form the reference frame of the complete model.

In addition, selected data of the following geodetic and geodynamics networks are used:

- Fifty three coordinate differences of the SIRGAS GPS campaigns 1995 and 2000, covering the entire South American continent (Drewes et al. 2005)
- Thirty one velocities of the CASA geodynamics project, Venezuela, 1988...2002 (Kaniuth et al. 2002a)
- Forty four velocities of the CASA geodynamics project, Costa Rica, Panama, Colombia, and Ecuador, 1991...1998 (Trenkamp et al. 2002)
- Twenty nine velocities of a local network within CASA around Cali, Colombia, 1996...2003 (Trenkamp et al. 2004)
- Sixty nine velocities of the integrated CAP-SNAPP project, Peru and Bolivia, 1993...2001 (Kendrick et al. 2001, 2003)
- Sixty eight velocities of the CAP geodynamics project, central Andes, 1993...2001 (Brooks et al. 2003)
- Thirty eight velocities of the SAGA geodynamics project, northern Chile, 1996...1997 (Khazaradze and Klotz 2003)
- Seventy nine velocities of the SAGA geodynamics project, central Chile, 1994...1996 (Klotz et al. 2001)
- Ten velocities of a geodetic project, central Chile, 2006...2008 (Baez et al. 2007)

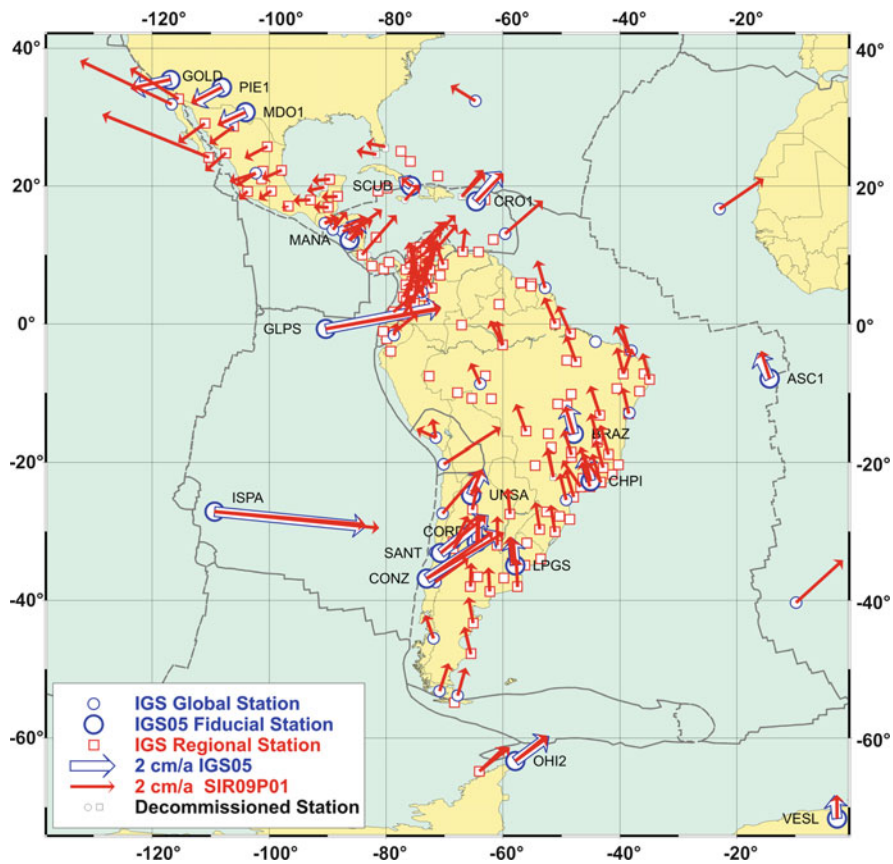

Fig. 81.1 Reference model SIR09P01 (Seemüller et al. 2009)

- Forty four velocities of a seismic gap network, southern Chile, 1996. . .2002 (Ruegg et al. 2009)
- Fifty four velocities of a deformation network, central Chile, 2004. . .2006 (Vigny et al. 2009)
- Twenty velocities of a Scotia-South America plate project, 1998. . .2001 (Smalley et al. 2003).

81.3 Data Processing

The velocities of all the regional data sets refer to different kinematic datums, i.e. they used different ITRF realizations or individual station velocities as the reference. Therefore, in the first step of data processing, velocities of all data sets were transformed to the continental solution SIR09P01 in the ITRF2005 datum by estimated spherical rotation vectors using identical points (most projects include IGS stations). They were then reduced to the South American plate by its plate rotation parameters in the ITRF2005 (Drewes 2009). If no identical points with SIR09P01 were available, stations overlapping with other projects were used. Identical stations in different projects were analysed w.r.t. reliability (number and length of observation periods, total time interval covered), and only one velocity per site was accepted. Doubtful velocities

Table 81.1 Velocities used for the modelling

Project	No. velocities
SIR09P01 as the reference frame	95
SIRGAS 1995. . .2000 differences	28
CASA (Venezuela)	21
CASA (Costa Rica . . . Ecuador)	31
CASA (Cali, Colombia)	17
CAP-SNAPP (Peru, Bolivia)	54
CAP (Central Andes)	60
SAGA 1996. . .1997 (Northern Chile)	32
SAGA 1994. . .1996 (Central Chile)	68
Scotia-South American plate boundary	19
Seismic gap (Southern Chile)	65
Chile (others)	6
Total	496

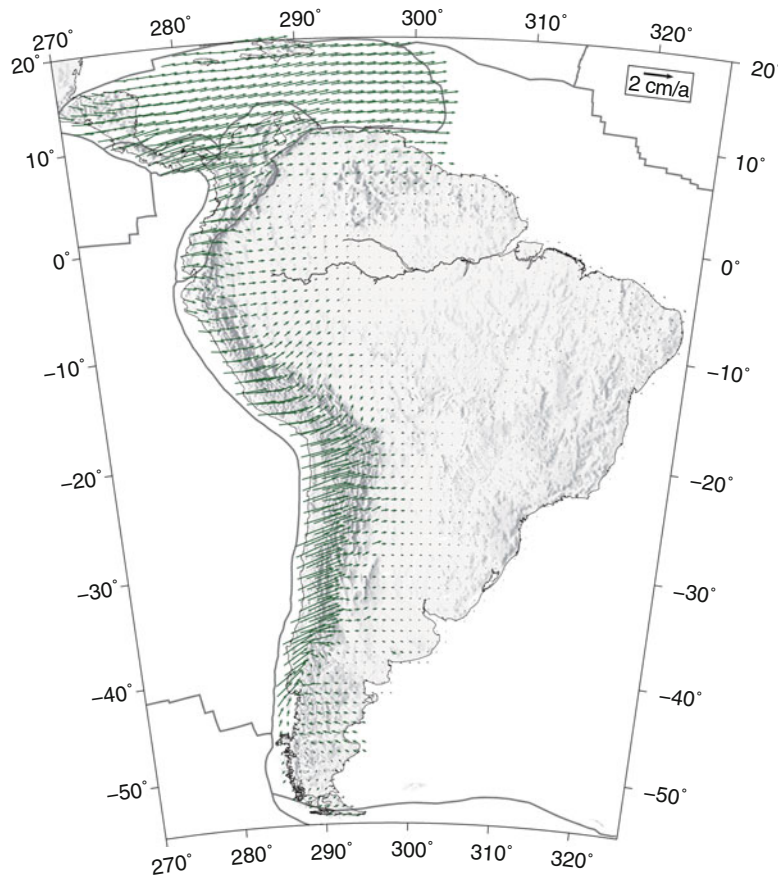

Fig. 81.2 Velocity field from finite element model

found in the comparisons were eliminated. In areas where earthquakes with considerable co-seismic station displacements occurred during the observation period, e.g. at Cariaco, Venezuela (Kaniuth et al. 2002a) and Arequipa, Peru (Kaniuth et al. 2002c), the seismic deformations were excluded from the velocity computations by using only pre-seismic observations. The complete set of final input data is listed in Table 81.1.

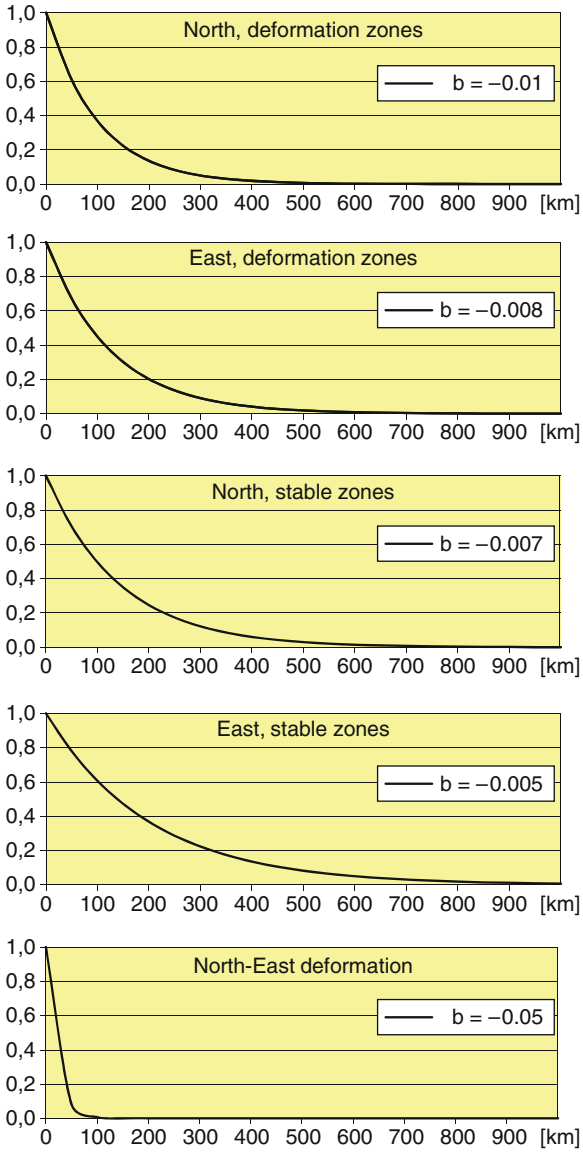

Fig. 81.3 Typical correlation functions of velocity North and East components and North-East cross correlations in deformation and stable zones

81.4 Finite Element Model

One possibility to estimate the continuous velocity field is to set up a geo-mechanical model with the observed velocities as boundary conditions. As the distribution of observation sites is very irregular, it is reasonable to use the finite element method for solving the numerical problem of partial differential equations of the equilibrium of forces. The two-dimensional model is approximated on a sphere with a radius of 6,371 km. The only further boundary condition is that the four corner sides are fixed in order to avoid rotation of the whole model. In contrast to the previous approach for that area presented in Drewes and Heidbach (2005), the implementation of the right-lateral Boconó – El Pilar fault system of Venezuela and Colombia is neglected because the velocities observed are purely from the inter-seismic phase, i.e. the fault is locked in this period. Thus, the implementation of a sliding fault does not meet the used data set. However, the impact of these local effects is rather small and does not change the results significantly.

The rheology of this geo-mechanical model is a homogeneous, isotropic, elastic (Hooke) material with Young's modulus $E = 70$ GPa and Poisson's ratio $\upsilon = 0.25$. The discretization of the model area consists of 500,000 plane strain linear elements, over which the deformation ε is computed in northern (N) and eastern (E) direction from the stress σ derived from the geodetic observations.

The basic equations read

$$\varepsilon_N = 1/E(\sigma_N - \upsilon\sigma_E) \tag{81.1a}$$

$$\varepsilon_E = 1/E(\sigma_E - \upsilon\sigma_N). \tag{81.1b}$$

To solve the numerical problem, the commercial finite element software package ABAQUS, version

Table 81.2 Typical parameters of empirical covariance functions for North- and East velocity components and North-East cross-correlation

	Deformation zones		Stable zones	
	a (cm/a)^2	b	a (cm/a)^2	b
North	0.10	−0.010	0.01	−0.007
East	0.60	−0.008	0.03	−0.005
N–E	0.11	−0.053	0.01	−0.007

6.9, was used. The result of the velocity field is displayed on a regular 1° grid and shown in Fig. 81.2.

81.5 Least Squares Collocation Approach

The least squares collocation approach was applied as a vector prediction using empirical covariance functions. The predicted continuous velocities are a function of the observed station velocities and the correlations between them:

$$\mathbf{v}_{\text{pred}} = \mathbf{c}_{\text{in}}^{\text{T}} \mathbf{C}_{\text{ij}}{}^{-1} \mathbf{v}_{\text{obs}}, \tag{81.2}$$

where $\mathbf{v}_{\text{obs}}$ is the observed velocity vector, $\mathbf{v}_{\text{pred}}$ the predicted vector, $\mathbf{C}_{\text{ij}}$ the auto-covariance matrix between the observed and $\mathbf{c}_{\text{in}}$ the covariance matrix between observed and predicted velocity vectors.

The elements of covariance matrices are taken from empirical isotropic covariance functions: one for each of the north and east velocity components and one for the cross correlation between the north and east components. Empirical correlations are computed in distance (d) classes between the points and approximated by simple exponential functions $a \cdot \exp(-b \cdot d)$. The distances d are computed on a sphere with a radius of 6,371 km. Typical examples of covariance functions are shown in Fig. 81.3 and summarized in Table 81.2. The parameters a and b vary for individual regions up to about 50% around the given mean value.

The figures clearly demonstrate that a uniform covariance function for all components cannot be applied. The correlation length in stable zones is significantly longer than in deformation zones, and the East component has a longer correlation than the North component. As expected, the cross-correlations between North and East components in deformation zones are very small. The use of these functions guarantees that the covariance matrices are always positive definite.

To get a sufficiently dense input velocity field, a wide-spaced grid is first interpolated in areas with sparse observations; in particular in the central part of the stable South American plate (Brazil). Only station

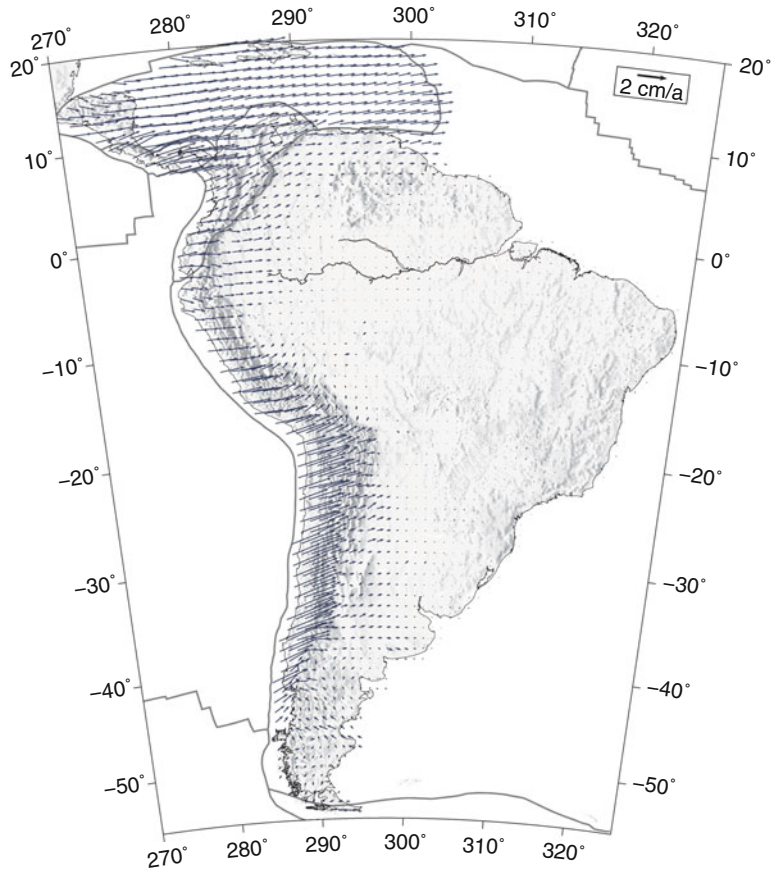

Fig. 81.4 Velocity field from least squares collocation

velocities of this region are used for this interpolation. These interpolated values are then included in the final prediction procedure. A $1^\circ \times 1^\circ$ grid covering the entire South American and Caribbean area is predicted by using estimated individual covariance functions from the surrounding observed velocities up to a distance of 2,000 km. The result is shown in Fig. 81.4. The formal prediction error of velocities varies, dependent on the region, from less than ± 1 mm/a up to ± 9 mm/a in the areas with sparse observation coverage.

81.6 Comparison of Finite Element and Least Squares Collocation Results

The comparison of results of the two approaches shows an agreement better than the formal precision of the individual methods. The deviations vary in the North component from -5 to +3.5 mm/a with an r.m.s. deviation of ± 0.8 mm/a. In the East component, where the velocity variation is greater, we have deviations between -6 and +6.3 mm/a and an r.m.s. deviation of ± 1.4 mm/a. A graphical impression of the differences is given in Fig. 81.5. The discrepancies are largest in zones with poor observation data, i.e., in the Caribbean Sea, where only a few islands have been observed, and the jungle areas in the eastern Andes of Colombia, Peru and Bolivia, as well as in Patagonia. The different interpolation methods of the finite element and least squares collocation methods become effective here. A decision regarding the superior reliability of the two methods cannot be made.

81.7 Comparison with the Previous Model

The main differences of the velocity field here presented and the formerly computed velocity field for South America (Drewes and Heidbach 2005) are the increased number of observations (496 instead of

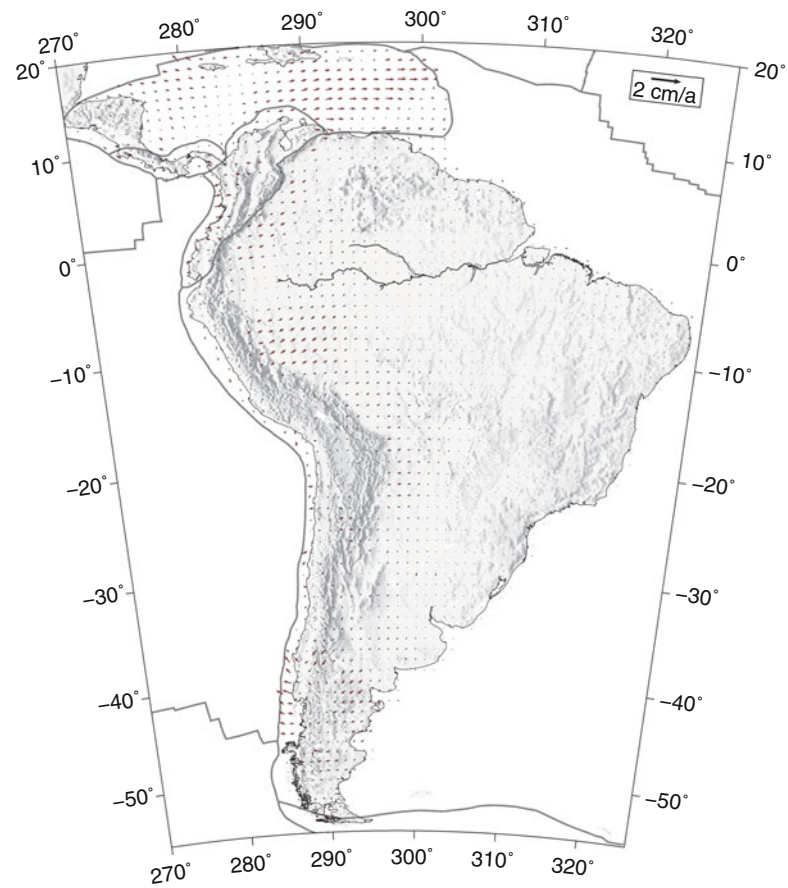

Fig. 81.5 Differences between finite elements and least squares collocation models

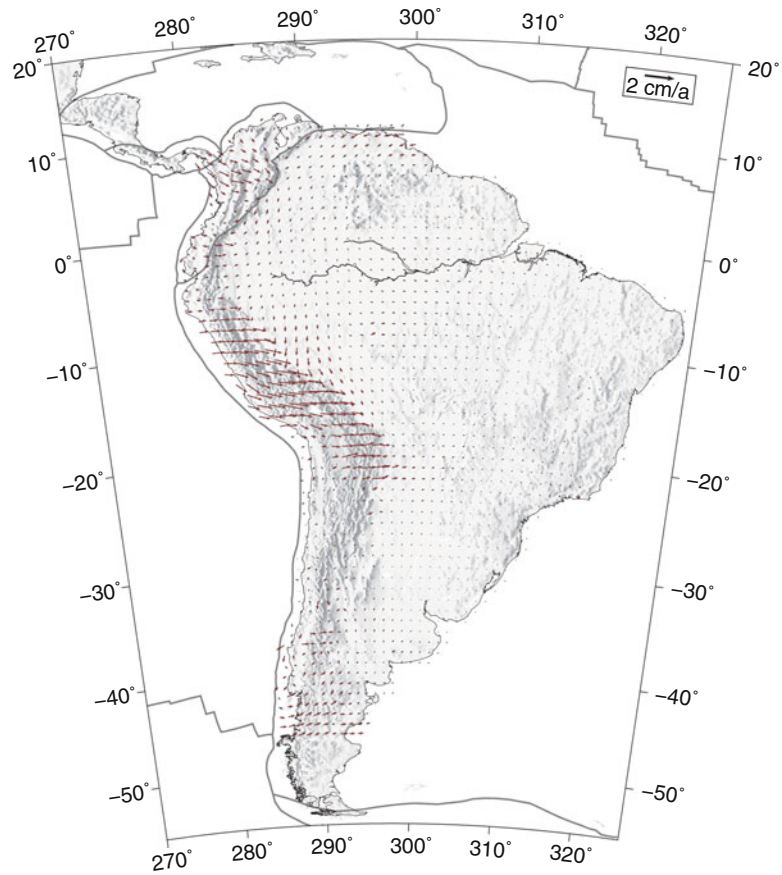

Fig. 81.6 Differences between 2009 and 2003 velocity fields

329), the better quality of measurements due to an increasing number of continuously observing GPS stations (included in SIR09P01), and the extension to the Caribbean and Tierra del Fuego (southern Argentina and Chile).

The differences of the two models shown in Fig. 81.6 vary between −8 and +3 mm/a in the North component and −9 to +18 mm/a in the East component. The r.m.s. deviations are ±1.3 mm/a in the North and ±3.2 mm/a in the East components. The largest discrepancies are found in the central Andes and in Colombia, where a large number of continuously observing GPS stations has recently come online.

Conclusions

The horizontal velocity model computed by finite element and least squares collocation approaches provides a continuous deformation model over the South American continent and the Caribbean. It can be used for interpolating point velocities arising from plate tectonic motions and Earth crust deformations, e.g. for transforming coordinates of newly installed geodetic stations from the observation epoch to the reference epoch of a given reference frame. The velocities shown here refer to the South America plate. For transformation to the ITRF2005 reference frame one has to add its global plate rotation (Drewes 2009). The corresponding plot and data file is available for practical use of interpolation at http://www.sirgas.org.

The velocity model presented here is not appropriate for any sophisticated analysis of geodynamic features and processes because no detailed crust and mantle models were set up. Furthermore, all the geodetic velocities included in the computations are inter-seismic data and, thus, do not necessarily represent the long-term average velocities needed for interpreting the tectonic evolution in the area.

The vertical velocity component was not included in the model, because its modelling cannot

be done in a continental scale without very detailed regional and local geophysical models. There are significant differences in vertical velocities over short distances, e.g. caused by fluid withdrawal (e.g. Drewes 1980) and/or subsidence of sediment basins (e.g. Kaniuth et al. 2002b; Kaniuth and Stuber 2005). Thus, the correlation length in least squares collocation is extremely short for vertical velocities and the finite element model requires a very dense network of discretization, variable Hooke parameters and boundary conditions. Such models on a local or regional scale are still to be developed and established.

References

Baez JC, de Freitas SRC, Drewes H, Dalazoana R, Luz RT (2007) Deformations control for the Chilean part of the SIRGAS 2000 frame. IAG Symposia, Springer, Berlin, vol 130, 660–664

Bird P (2003) An updated digital model for plate boundaries. Geochem Geophys Geosyst 4 No. 3, p 52, doi:1010.1029/2001GC000252

Brooks BA, Bevis M, Smalley R, Kendrick E, Manceda R, Lauria E, Maturana R, Araujo M (2003) Crustal motion in the southern Andes (26°–36°S): Do the Andes behave like a microplate? Geochem Geophys Geosyst GC000505

DeMets C, Gordon RG, Argus DF, Stein S (1990) Current plate motions. Geophys J Int 101:425–478

DeMets C, Gordon R, Argus DF, Stein S (1994) Effect of recent revisions to the geomagnetic reversal time scale on estimates of current plate motions. Geophys Res Lett 21:2191–2194

Drewes H (1980) Precise Gravimetric Networks and Recent Gravity Changes in Western Venezuela. Dt. Geod. Komm., Reihe B, Nr. 251, München

Drewes H (2009) The Actual Plate Kinematic and crustal deformation Model (APKIM2005) as basis for a non-rotating ITRF. Springer, IAG Symposia, vol 134, 95–99 doi:10.1007/978-3-642-00860-3_15

Drewes H, Kaniuth K, Voelksen C, Alves Costa SM, Fortes LPS (2005) Results of the SIRGAS campaign 2000 and coordinates variations with respect to the 1995 South American geocentric reference frame. IAG Symposia, Springer, Berlin, vol 128, 32–37

Drewes H, Heidbach O (2005) Deformation of the South American crust estimated from finite element and collocation methods. IAG Symposia, Springer, Berlin, vol 128, 544–549

Espurt N, Funiciello F, Martinod J, Guillaume B, Regard V, Faccenna C, Brusset S (2008) Flat subduction dynamics and deformation of the South American plate: Insights from analog modeling. Tectonics (27) TC3011, doi:10.1029/2007TC002175

Heidbach O, Iaffaldano G, Bunge H-P (2008) Topography growth drives stress rotations in the central Andes: Observations and models. Geophys Res Lett (35) L08301, 6pp, doi:10.1029/2007GL032782

Kaniuth K, Drewes H, Tremel H, Stuber K, Kahle H-G, Geiger A, Hernandez JN, Hoyer MJ, Wildermann E (2002a). Interseismic, co-seismic and post-seismic deformations along the South American-Caribbean plate boundary from repeated GPS observations in the CASA project. Proceedings of the IAG Symposium "Recent crustal deformations in South America and surrounding area", Santiago, Chile

Kaniuth K, Haefele P, Sanchez L (2002b) Subsidence of the permanent GPS station Bogota. IAG Symposia, Springer, Berlin, vol 124, 56–59

Kaniuth K, Mueller H, Seemueller W (2002c) Displacement of space geodetic observatory Arequipa due to recent earthquakes. Zeitschr für Verm 127:238–243

Kaniuth K, Stuber K (2005) Apparent and real local movements of two co-located permanent GPS stations at Bogota, Colombia. Zeitschr für Verm 130:41–46

Kendrick E, Bevis M, Smalley R, Brooks B (2001) An integrated crustal velocity field for the central Andes. Geochem Geophys Geosyst 2:2001GC000191

Kendrick EC, Bevis M, Smalley R (2003) The Nazca – South America Euler vector and its rate of change. J South Am Earth Sci 16:125–131

Khazaradze G, Klotz J (2003) Short- and long-term effects of GPS measured crustal deformation rates along the south central Andes. J Geophys Res 108(B6):5, 15

Klotz J, Khazaradze G, Angermann D, Reigber C, Perdomo R, Cifuentes O (2001) Earthquake cycle dominates contemporary crustal deformation in Central and Southern Andes. Earth Planet Sci Lett 193:437–446

Ruegg JC, Rudloff A, Vigny C, Madariaga R, de Chabalier JB, Campos J, Kausel E, Barrientos S, Dimitrov D (2009) Interseismic strain accumulation measured by GPS in the seismic gap between Constitución and Concepción in Chile. Phys Earth Planet Int 175:78–85

Seemüller W, Seitz M, Sánchez L, Drewes H (2009) The position and velocity solution SIR09P01 of the IGS Regional Network Associate Analysis Centre for SIRGAS (IGS RNAAC SIR). DGFI Report No. 85, available at http://www.sirgas.org/ and this volume

Smalley R, Kendrick E, Bevis MG, Dalziel IWD, Taylor F, Lauria E, Barriga R, Casassa G, Olivero E, Piana E (2003) Geodetic determination of relative plate motion and crustal deformation across the Scotia-South America plate boundary in eastern Tierra del Fuego. Geochem Geophys Geosyst (4) No. 9, doi:10.1029/2002GC000446

Trenkamp R, Kellogg JN, Freymueller JT, Mora HP (2002) Wide margin deformation, southern Central America and northwestern South America, CASA GPS observations. J South Am Earth Sci 15:157–171

Trenkamp R, Mora H, Salcedo E, Kellogg JN (2004) Possible rapid strain accumulation rates near Cali, Colombia, determined from GPS measurements (1996–2003). Earth Sci Res J 8:25–33

Vigny C, Rudloff A, Ruegg J-C, Madariaga R, Campos J, Alvarez M (2009) Upper plate deformation measured by GPS in the Coquimbo Gap, Chile. Phys Earth Planet Int 175:86–95